Appl Biochem Biotechnol (2013) 171:1405–1415
DOI 10.1007/s12010-013-0429-2

Quenching Action of Monofunctional Sulfur Mustard on Chlorophyll Fluorescence: Towards an Ultrasensitive Biosensor

Simerjit Kaur · Minni Singh · Swaran Jeet Singh Flora

Received: 15 June 2013 / Accepted: 5 August 2013 /
Published online: 18 August 2013

Abstract An ultrasensitive fluorimetric biosensor for the detection of chemical warfare agent sulfur mustard (SM) was developed using its monofunctional analogue. SM is a vesicant and a potent chemical threat owing to its direct toxic effects on eyes, lungs, skin and DNA. This work investigates the quenching action of the analyte on chlorophyll fluorescence as elucidated by nuclear magnetic resonance, Fourier transform infrared spectroscopy and mass spectrometry studies suggesting the electrophilic attack of carbonium ion on nitrogens of the porphyrin moiety of chlorophyll. The properties of immobilisation matrix were optimised and scanning electron microscope observations confirmed improvement in pore size of sol–gels by addition of 32 % (*v*/*v*) glycerol, a feature enabling enhanced sensitivity towards the analyte. Chlorophyll embedded sol–gel was treated with increasing concentrations of monofunctional SM and the corresponding drop in maximum fluorescence intensity as measured by emission at 673 nm was observed, which varied linearly and had a detection limit of 7.68×10^{-16} M. The biosensor was found to be 6 orders of magnitude more sensitive than the glass microfibre-based disc biosensor previously reported by us.

Keywords Biosensor · Fluorescence · Sulfur mustard · Sol–gel · Ultrasensitive

Introduction

Among the nuclear, biological and chemical weapons of mass destruction, chemical warfare agents (CWAs), which are broadly classified into choking agents, blood agents, blistering agents and nerve agents are most accessible, thereby posing a serious threat particularly to developing nations [1]. Severely antisocial activities such as the release of bioterror agents like *Bacillus anthracis* and ricin have threatened world communities. More recently, confirmed reports of

S. Kaur · M. Singh (✉)
Biosensor Development Laboratory, Department of Biotechnology, Punjabi University, Patiala 147002 Punjab, India
e-mail: minnisingh@pbi.ac.in

S. J. S. Flora
Division of Regulatory Toxicology, Defence Research and Development Establishment, Jhansi Road, Gwalior 474002, India

mustard gas stockpiles in war afflicted nations, as reported by Organisation for the Prohibition of Chemical Weapons, has raised concern [2, 3]. Following these, it has been feared that antisocial groups might be attracted towards using chemical weapons of mass destruction like sulfur mustard and sarin. It is, therefore, incumbent for nations to monitor the presence of CWAs, which would require detection of these toxic agents at subnanomolar concentrations.

Sulfur mustard [SM, *bis*(2-chloroethyl)sulfide, $C_4H_8Cl_2S$] is a blistering and alkylating agent used in warfare that has severe physiological implications rendering it a potent chemical weapon [4]. There is extensive ongoing research on its mechanism of action, decontamination and development of antidotes for treatment of SM-induced injuries [5–7]. Conventional techniques for SM detection include matrix-assisted laser desorption/ionization time-of-flight mass spectrometry (MS), gas chromatography and liquid chromatography [8–10]. These techniques are laboratory bound and require extensive sample pre-treatment besides lower sensitivity, which authenticates the demand for alternate methods of detection. Sensors such as quartz crystal microbalance sensors, polymer-based surface acoustic wave sensor arrays and electrochemical sensors have been developed for SM which offer sensitive detection down to nanomolar concentrations [11–16]. Biosensors have emerged as promising analytical tools in the past decade which have the ability to offer ultrasensitive subnanomolar detection of analytes, besides ease of use and negligible sample treatments. To the best of our knowledge, there are three reports on biosensors for SM till date. One utilises the suppression of induced fluorescence as a fluorimetric detecting phenomenon, altering the photosystem II (PS II) efficiency of living photosynthetic microorganisms *Nostoc commune* and *Chlorella vulgaris* and exhibits a detection limit of 2.87 μM for SM analogue, dibutyl sulfide [17]. The other work reported piezoelectric detection using antigen-antibody specific interaction using polyclonal and monoclonal anti-SM antibodies produced with carrier proteins. However, authors reported this to be a preliminary study as the concentration of SM used was very high [18]. The most recent report is our work which utilises the fluorescing ability of chlorophyll as the biorecognition element which was immobilised on glass microfibre discs coupled to an optical transducer. Drop in fluorescence was observed upon exposure to 2-chloroethyl ethyl sulfide (2-CEES), SM analogue, which varied linearly with increasing 2-CEES concentrations and exhibited a detection limit of 7.68×10^{-10} M. This drop in maximum fluorescence intensity (F_{max}) was attributed to conversion of chlorophyll into its breakdown products as suggested by high-performance liquid chromatography profiles [19]. However, the complete elucidation of mechanism remained to be studied. Therefore, in an endeavour to develop an ultrasensitive optical biosensor owing to the toxic nature of the analyte, the present investigation has been undertaken with an aim to elucidate the fluorescence quenching mechanism of monofunctional SM and its nature of interaction with chlorophyll.

Material and Methods

Material

Colloidal silica, Ludox® HS 40 and 2-CEES, purity 98 %, were purchased from Sigma-Aldrich (St. Louis, MO, USA). Fluorescing biomolecule–chlorophyll: source, green leaves of *Hibiscus rosa-sinensis*. Solvents and other analytical grade chemicals were purchased from Merck and HiMedia, Mumbai, India. Stock solution of 2-CEES in methanol was stored in dark at 4 °C. Chlorophyll extract was prepared fresh in petroleum ether and redissolved in methanol owing to its favourable aqueous polarity for subsequent development of biosensor. All bench experiments were performed under dim light conditions.

Chlorophyll Fluorescence Induction

Excitation (λ_{ex}) and emission (λ_{em}) wavelength of chlorophyll were identified by recording its fluorimetric spectra on a Varian Cary eclipse fluorescence spectrophotometer for which chlorophyll was extracted from green leaves of *H. rosa-sinensis* and quantified according to Ranganna [20]. All further fluorescence studies were done on digital photofluorometer EI 681 using a 50 W tungsten halogen lamp as a light source via a shutter and a broad band interference transmitting through primary corning 5113 filter and collecting the emission through secondary corning 3385 filter detected with a sensitive wide-range photodiode. Chlorophyll was induced to F_{max} by varying flash/dark time cycles.

2-CEES as a Fluorescence Quencher

To study the effect of 2-CEES on fluorescence, which is the underlying sensing phenomenon for the development of this optical biosensor, the biomolecule was flash induced with 10-s flash/2 min dark cycle and a subsequent drop in F_{max} upon treatment with 2-CEES, if any, was observed. To explicate the quenching phenomenon proton nuclear magnetic resonance spectroscopy (^{1}H NMR) and Fourier transform infrared spectroscopy (FTIR) spectra of 2-CEES treated chlorophyll were recorded on Bruker Avance II 400 magnetic resonance spectroscopy (NMR) spectrometer operating at 400 MHz and Perkin Elmer Spectrum 400 FTIR spectrophotometer, respectively. Our findings were further corroborated by recording a mass spectrum on Thermoscientific LTQXL mass spectrometer with electron spray ionisation source in positive ion mode with a source voltage of 3 kV.

Biosensor Preparation

Due to optical-based transduction, sol–gel matrix was opted for immobilisation of chlorophyll. For this, colloidal silica, the precursor was initiated towards gelation by addition of H^+ and Na^+ ions. To attain high sensitivity of detection, varying concentrations of glycerol were added into the matrix and the gel porosity was characterised by scanning electron microscope (SEM) studies. Scanning electron micrographs were captured on a JEOL-JSM-6610LV scanning electron microscope at an accelerating voltage of 15 kV after gold coating. One hundred microliter sols containing 19.2 % silica, 0.1 M NaCl and chlorophyll (0.24–2.4 μg) were cast onto a 96-well microtitre plate for 8.25 h to allow complete gelation. Thereafter, gels embedded with 2.4 μg chlorophyll were treated with increasing concentrations of 2-CEES after induction and a subsequent drop in F_{max} was observed to identify a linear range of detection.

Results and Discussion

Chlorophyll Induction to Maximum Fluorescence Intensity

The total chlorophyll extract exhibited λ_{ex} and λ_{em} at 442 and 673 nm, respectively. To attain a high sensitivity of response the biomolecule was induced to F_{max} by high energy photons, exciting the electrons in the reaction centre of PS II which upon relaxation emit long wave radiation as fluorescence (refer to Fig. 4). It was observed that with 10-s flash/5 min dark time cycle, F_{max} was attained after 1 h which may be attributed to prolonged dark time. On the other hand, 10-s flash/2 min dark time cycle yielded a distinctive F_{max} at 2 min, a combination thereby chosen for chlorophyll fluorescence induction (data not shown).

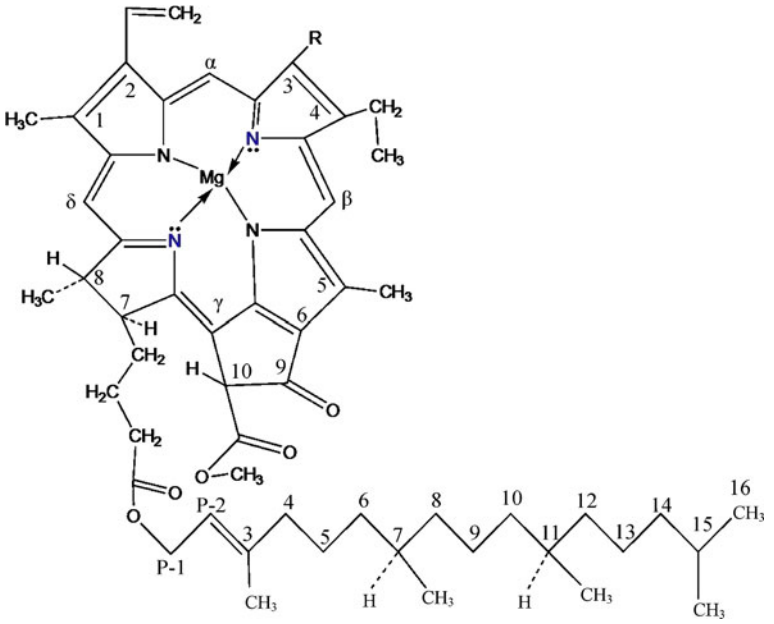

Fig. 1 Structure of chlorophyll

2-CEES as a Fluorescence Quencher

The fluorescence quenching action of SM has been under investigation by many workers. The studies focus around the electrophilic sulfur atom and the alkyl group. The present work is an endeavour to elucidate the mechanism of SM action on chlorophyll, the fluorescing

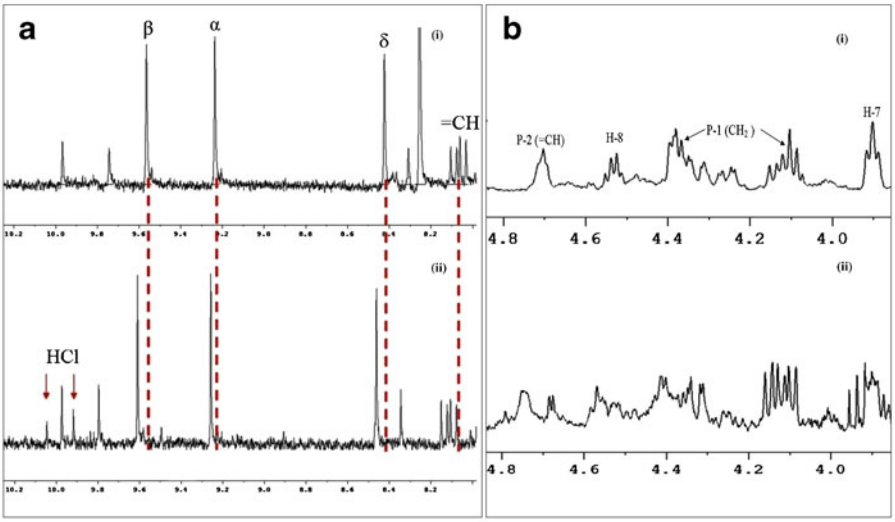

Fig. 2 ^{1}H NMR spectra of **a** porphyrin moiety of chlorophyll *i* before treatment and *ii* after treatment with 2-CEES; **b** phytol region *i* before treatment and *ii* after treatment with 2-CEES

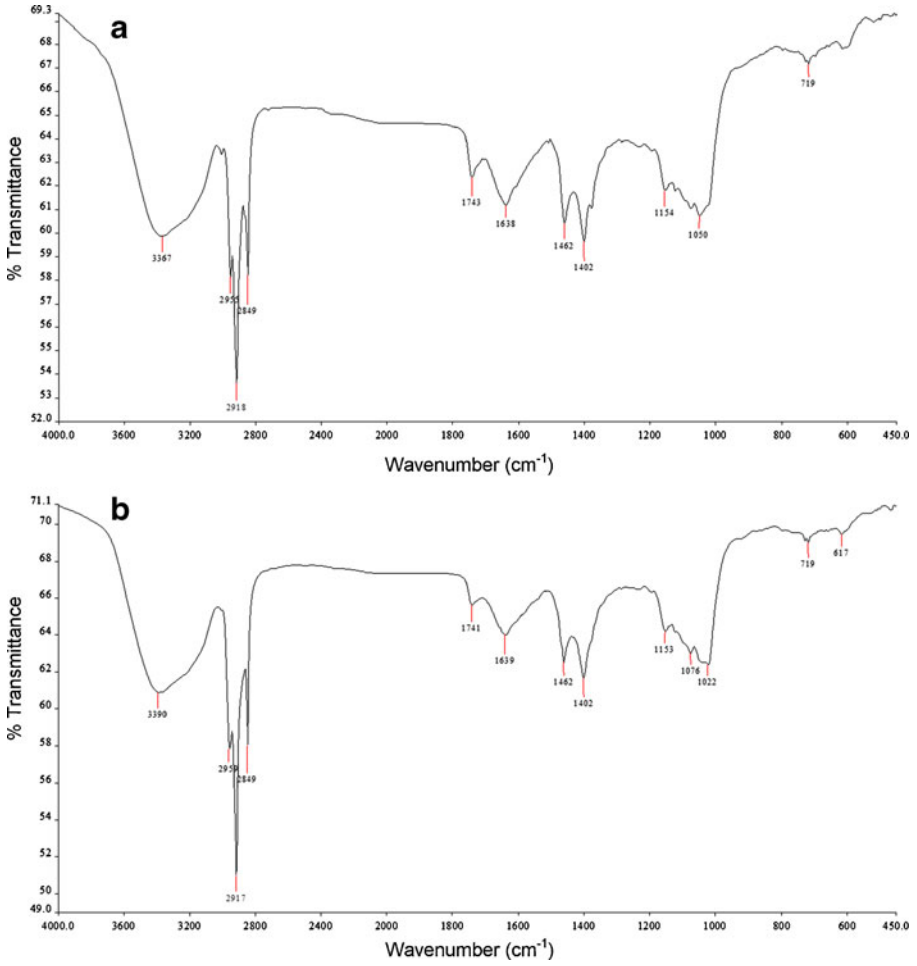

Fig. 3 FTIR spectra of chlorophyll **a** before treatment and **b** after treatment with 2-CEES

biomolecule. The structure of chlorophyll is shown in Fig. 1. As expected, treatment of flash-induced chlorophyll with monofunctional SM showed an inhibitory effect on F_{max}, higher concentrations leading to an increased drop in maximum fluorescence intensity (data for free system not shown).

The ^{1}H NMR spectra of chlorophyll before and after treatment with 2-CEES is shown in Fig. 2. Figure 2a (i and ii) are the ^{1}H NMR spectra of porphyrin moiety of chlorophyll whereas, Fig. 2b (i and ii) represent the spectra of the phytol region, the two regions which are significantly affected by 2-CEES. Resonance values to individual protons were assigned according to Smith et al. [21]. Proton signals at δ 9.56, 9.21, 8.41 and 8.08 account for β, α, δ methine and =CH vinyl protons, respectively, which upon treatment with the analyte showed a significant downfield shift. This downfield shift may be attributed to the interaction of electron withdrawing groups of 2-CEES with porphyrin moiety of chlorophyll suggesting a possible bond formation discussed subsequently. One of the leading works by Fujimori [22] on the action of SM on fluorescing molecules suggested that the alkyl group of the analyte was responsible for fluorescing quenching. On the contrary, Hunt and

Table 1 Position and assignments of bands in FTIR spectra

Chlorophyll (cm^{-1})	2-CEES treated chlorophyll (cm^{-1})	Assignment
3,367	3,390	N–H stretching (aromatic)
2,955, 2,918, 2,849	2,959, 2,917, 2,849	C–H stretching (alkanes)
1,743	1,741	C=O stretching (ester)
1,638	1,639	C=C stretching (alkene aliphatic)
1,462, 1,402	1,462, 1,402	C–C stretching (aromatic)
1,154, 1,076, 1,050	1,153, 1,076	C–O stretching (ester)
	1,022	C–N stretching
719	719	C–H deformation (aromatic)

Alder [23] suggested that the competitive reacting component is sulfide; however, their NMR studies were inconclusive.

Under mild aqueous conditions, 2-CEES forms a cyclic transient ethylene sulfonium cation via SN_1 intramolecular assistance of neighbouring sulfur atom with the loss of Cl^-, generating HCl, thereby rendering it a blistering agent [24, 25]. Based on our observation, we suggest that the transient intermediate sulfonium ion undergoes rearrangement to form more stable carbonium ion which is followed by its electrophilic attack on the nitrogens within the porphyrin ring of chlorophyll during which intramolecular energy transfer takes place facilitating the non-radiative transitions to ground state resulting in fluorescence quenching. This is supported by similar action of SM on nitrogen-7 of guanine and nitrogen-3 of adenine of the DNA [26]. Subsequent FTIR and MS studies will confirm the observation. The appearance of two signals at δ 9.91 and 10.06 can be ascribed to the protons of HCl generated by 2-CEES. The action of HCl on chlorophyll leads to formation of pheophytin (refer to Fig. 4). Signals of protons attached to two nitrogens after the loss of central magnesium atom appear at δ 9.79 and 9.98.

In Fig. 2b (i) proton signals at δ 3.9, 4.54, (4.10, 4.38) and 4.7 are assigned to H-7, H-8, P-1 (CH_2) and P-2 (=CH) protons, respectively, where prefix-P stands for phytol chain protons which showed changes in their peak patterns after 2-CEES treatment, due to its conversion into pheophorbide and non-fluorescing catabolites causing changes in the proton environment after separation of phytol chain. Figure 3 shows the FTIR spectra of chlorophyll, showing characteristic bands of the biomolecule.

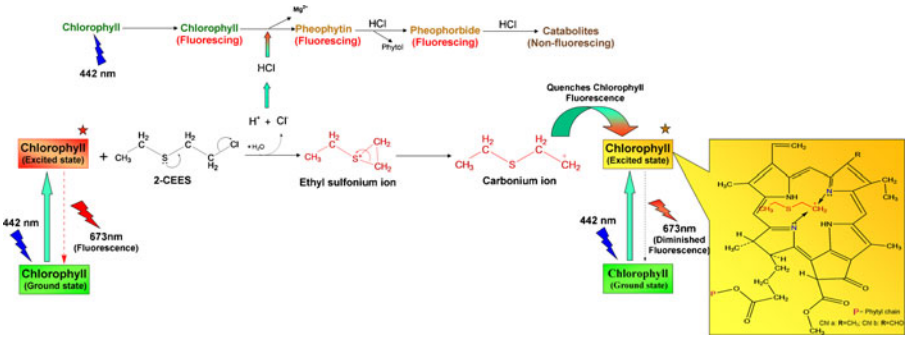

Fig. 4 Fluorescence quenching phenomenon of 2-CEES

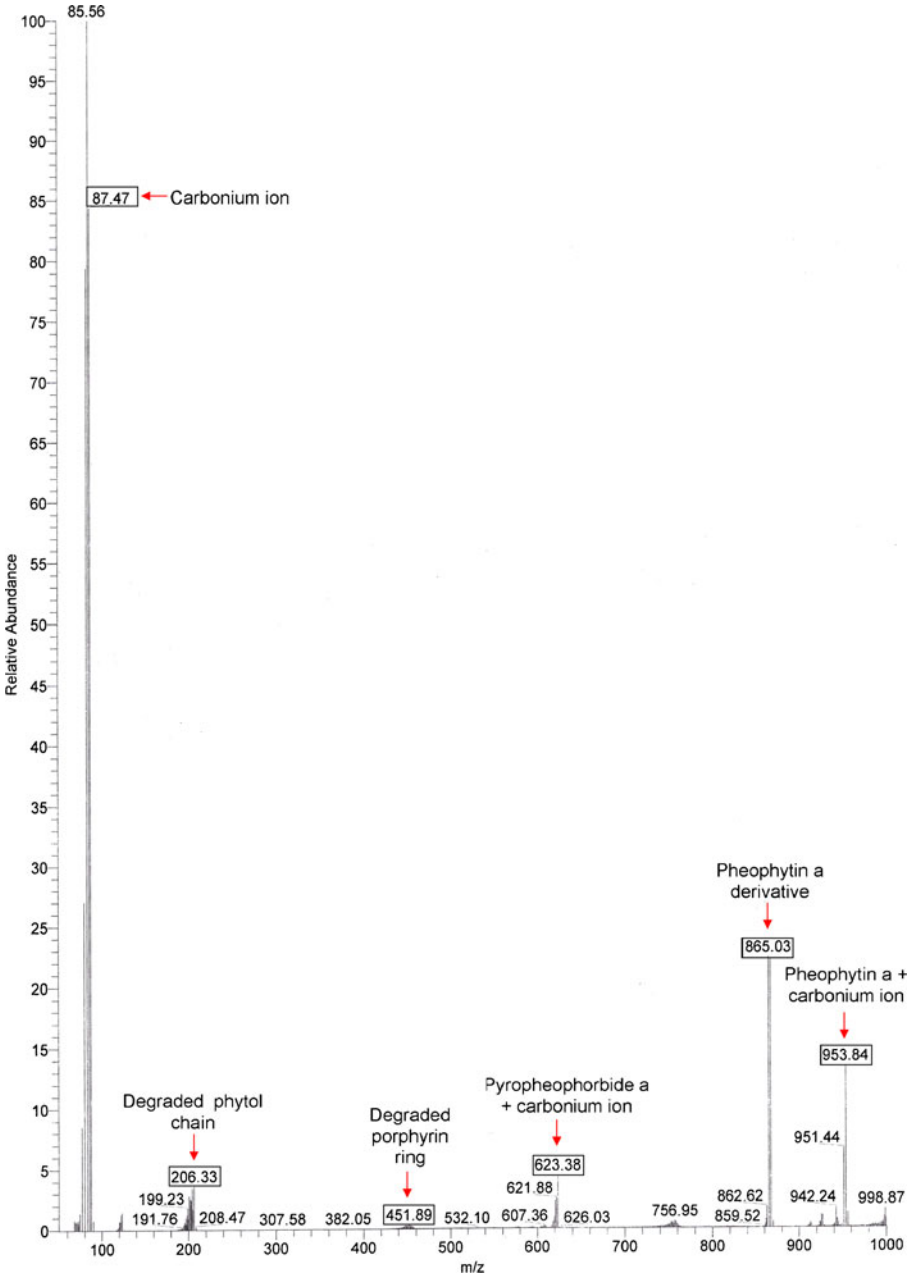

Fig. 5 Mass spectra of chlorophyll after 2-CEES treatment

Probable assignments of the bands are given in Table 1. The appearance of a new band at 1,022 cm^{-1} after 2-CEES treatment corresponds to C–N stretching thereby confirming bond formation between carbonium ion of 2-CEES and nitrogen of chlorophyll molecule. Further to that, a significant shift of N–H stretching peak from 3,367 to 3,390 cm^{-1} indicates the harbouring

Table 2 Effect of NaCl concentration on gelation. Concentration of silica used was 10.66 % (*w*/*v*)

NaCl concentration (M)	Gelation time	Observation
0.10	2 days 3 h 20 min ± 45 min	Transparent
0.25	8 h 20 min ± 15 min	Turbid
0.50	1 h 15 min ± 7.64 min	Turbid
0.75	25 min ± 5 min	Turbid
1.00	13 min ± 2.52 min	Turbid

of the analyte within the porphyrin moiety. The proposed action of 2-CEES as a chlorophyll fluorescence quencher is illustrated in Fig. 4.

Our elucidations were further confirmed with MS studies. Figure 5 shows the mass spectrum of chlorophyll after 2-CEES treatment. Major fragment ion was of ethylene carbonium ion at m/z=87.47. Fragment at m/z=865.03 corresponds to a pheophytin derivative formed by the action of HCl. The ion of m/z=953.84 [865.03+88.6 (carbonium ion)] confirms the interaction of 2-CEES with the chlorophyll molecule responsible for its fluorescence quenching. Fragment ion at m/z=623.38 [pyropheophorbide (534) +88.6] is due to further degradation of chlorophyll. Fragment ions at m/z=206.33 and 451.89 correspond to phytol chain and porphyrin moiety catabolic products, respectively.

Optical Biosensor Based on Fluorescence Quenching

The optical detection necessitated use of a transparent immobilisation matrix for biosensor development and silica sol–gels were used in this study. Ludox® HS 40 is a hydroxy stabilised 40 % (*w*/*v*) aqueous silica suspension. Hydroxyl ions render a high negative charge on silica accounting for its electrostatic stability. It is the destabilisation of this colloidal suspension that leads to aggregation and gelling. The destabilisation is brought about by changing its ionic environment by lowering the pH to 5.0–6.0 and by addition of salts like NaCl, KCl, LiCl and CsCl leading to diminution of repulsive forces causing aggregation [27]. In this work, gelation was done sequentially by: (a) lowering the pH to 7.0, thereby causing partial charge shielding (chlorophyll retains stability at near neutral conditions, lowering the pH below 7.0 is known to degrade the biomolecule, refer to Fig. 4); (b) addition of Na^+ ions. Na^+ ions catalyse gelation by

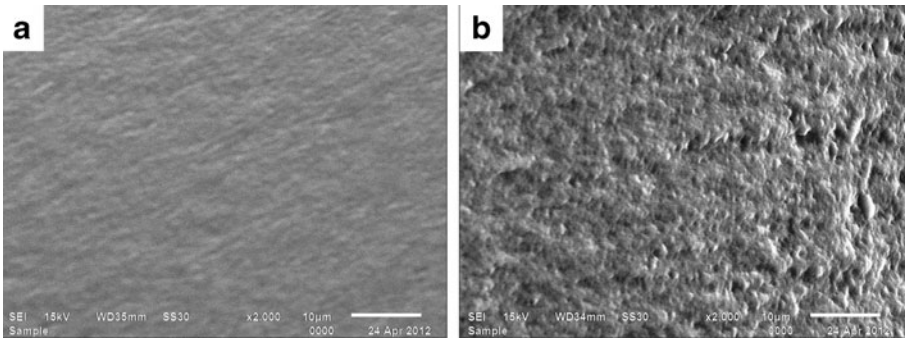

Fig. 6 SEM micrographs of gels containing **a** 4 % (*v*/*v*) glycerol and **b** 32 % (*v*/*v*) glycerol. Concentration of silica used was 19.2 % (*w*/*v*)

Table 3 Effect of silica concentration on gelation. Concentration of glycerol and NaCl used was 32 % (*v*/*v*) and 0.1 M, respectively

Silica concentration (%)	Gelation time	Observation
10.66	1 day 23 h 15 min ± 42.52 min	Transparent
13.70	22 h ± 22.91 min	Transparent
16.00	18 h ± 17.62 min	Transparent
17.85	15 h ± 15.28 min	Transparent
19.20	8 h 15 min ± 12.12 min	Transparent

providing electrostatic shielding of remaining partial negative charge on silica and by ion exchange between Na^+ and hydrogens of silanol groups [28]. Increased Na^+ ion concentration leads to loss of optical transparency which is due to an increase in fractal dimension of sol due to shielding of Coulombs interaction by Na^+ ions [29]. Due to this, both electrostatic potential and Debye shielding length decrease leading to an increase in van der Waals attraction between silica particles facilitating their aggregation and gelation. The effect of Na^+ (0.1–1.0 M NaCl) on optical transparency and gelation time was observed (Table 2), based on which 0.1 M NaCl was chosen for further studies.

Glycerol is known to increase the pore size of gels [30]. The porosity of gels with increasing concentrations of glycerol was measured (data not shown). SEM micrographs of gels with 4 and 32 % (*v*/*v*) glycerol are shown in Fig. 6, which clearly indicate the increased pore size with higher concentration of glycerol. The improved pore size facilitates greater interaction between embedded chlorophyll and 2-CEES both through micropores and macropores improving the sensitivity characteristics of the biosensor.

The effect of increasing silica concentration on gelation time was observed (Table 3) increasing concentration leading to faster gelation. Based on this, gels with 32 % (*v*/*v*) glycerol and 19.2 % (*w*/*v*) silica were selected for immobilisation of the biocomponent owing to faster gelation, larger pore size and adequate transparency.

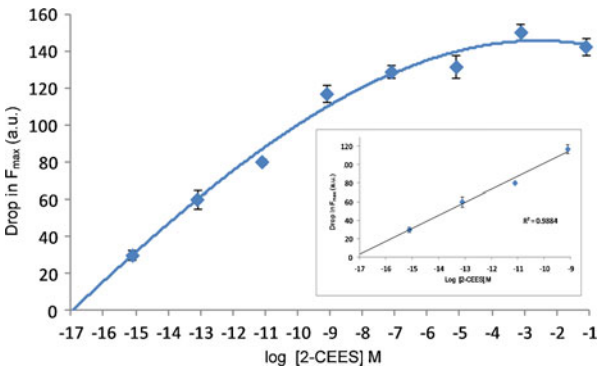

Fig. 7 Decrease in the fluorescent signal with increasing 2-CEES concentrations. The curve was fitted to a quadratic polynomial equation; *error bars* standard deviation from three independent measurements. The *inset* shows the linear variation of drop in F_{max} at lower 2-CEES concentrations

Biosensor Response to 2-CEES

F_{max} increases with increasing chlorophyll concentration, with maximum being attained with 2.4 μg/100 μl. To observe the drop in F_{max}, 2.4 μg chlorophyll embedded sol–gels were treated with increasing 2-CEES concentrations as shown in Fig. 7. From the figure, it is clear that the biosensor exhibits a limit of detection of 7.68×10^{-16} M and there is a saturation in response from 7.68×10^{-8} M onwards. The biosensor affords ultrasensitive detection of the said analyte when compared with previous works.

Conclusions

In conclusion, a fluorimetric biosensor was developed for sulfur mustard using its monofunctional analogue, 2-CEES. The sensor exhibits a detection limit of 7.68×10^{-16} M. We describe the mechanism of action of 2-CEES as a quencher of chlorophyll fluorescence. The ultrasensitive response is a promising feature of the biosensor. More so, the assay is a simpler alternative to existing sophisticated methods of detection. Our future work would focus on selective detection of SM with possible use of specific polymers.

Acknowledgments The authors thank the Defence Research and Development Establishment (DRDE), Gwalior, Ministry of Defence, Government of India for funding the research work. We are also thankful to IIT, Ropar; NIPER, Mohali and CIL, Punjab University, Chandigarh for providing some of the necessary facilities. We thank Dr. Vikrant Naik, postdoctoral fellow, Department of Materials, ETH Zurich for necessary inputs.

References

1. Ganesan, K., Raza, S. K., & Vijayaraghavan, R. (2010). *Journal of Pharmaceutical and Bioallied Sciences, 2*, 166–178.
2. Gaddafi could turn to Libya's mustard gas stockpile, some officials fear 2011. www.washingtonpost.com. Accessed 9 June 2013
3. Fears Gadafy may use mustard gas 2011. www.irishtimes.com. Accessed 11 June 2013
4. Toxicological profile for sulfur mustard (update) 2003. www.atsdr.cdc.gov. Accessed 9 June 2013
5. Tewari-singh, N., Gu, M., Agarwal, C., White, C. W., & Agarwal, R. (2010). *Chemical Research in Toxicology, 23*, 1034–1044.
6. Singh, R., Gutch, P. K., & Mazumder, A. (2013). *Industrial and Engineering Chemistry Research, 52*, 4689–4694.
7. Pino, M. A., Pietka-Ottlik, M., & Billack, B. (2013). *Arhiv za Higijenu Rada i Toksikologiju, 64*, 77–86.
8. Price, E. O., Smith, J. R., Clark, C. R., Schlager, J. J., & Shih, M. L. (2000). *Journal of Applied Toxicology, 20*, S193–S197.
9. Hooijschuur, E. W. J., Kientz, C. E., Hulst, A. G., & Brinkman, U. A. T. (2000). *Analytical Chemistry, 72*, 1199–1206.
10. Kimm, G. L., Hook, G. L., & Smith, P. A. (2002). *Journal of Chromatography A, 971*, 185–191.
11. Bunkar, R., Vyas, K. D., Rao, V. K., Kumar, S., Singh, B., & Kaushik, M. P. (2010). *Sens Tranducers, 113*, 41–47.
12. Zhang, Z., Fan, J., Yu, J., Zheng, S., Chen, W., Li, H., Wang, Z., & Zhang, W. (2012). *ACS Applied Materials & Interfaces, 4*, 944–949.
13. Matatagui, D., Fontecha, J., Fernandez, M. J., Aleixandre, M., Gracia, I., Cane, C., & Horrillo, M. C. (2011). *Talanta, 85*, 1442–1447.
14. Matatagui, D., Marti, J., Fernandez, M. J., Fontecha, J. L., Gutierrez, J., Gracia, I., Cane, C., & Horrillo, M. C. (2011). *Sensors and Actuators B: Chemical, 154*, 199–205.

15. Diakowski, P. M., Xiao, Y., Petryk, M. W. P., & Kraatz, H.-B. (2010). *Analytical Chemistry, 82*, 3191–3197.
16. Singh, V. V., Nigam, A. K., Boopathi, M., Pandey, P., Singh, B., & Vijayaraghavan, R. (2012). *Sensors and Actuators B: Chemical, 161*, 1000–1009.
17. Sanders, C. A., Rodriguez, M., Jr., & Greenbaum, E. (2001). *Biosensors and Bioelectronics, 16*, 439–446.
18. Skladal, P., Pribyl, J., & Safar, B. (2007). *Analytical Letters, 40*, 1347–1359.
19. Kaur, S., Singh, M. and Verma, N. (2012) IEEE 87–91
20. Ranganna, S. (2005). *Handbook of analysis and quality control for fruit and vegetable products* (2nd ed.). New Delhi: McGraw-Hill.
21. Smith, K. M., Goff, D. A., & Abraham, R. J. (1984). *Organic Magnetic Resonance, 22*, 779–783.
22. Fujimori, E. (1950). *Nippon Kagaku Zasshi, 71*, 471.
23. Hunt, A. L., & Alder, J. F. (1999). *Analitica Chimica Acta, 387*, 207–215.
24. Sugendran, K., Kumar, P., & Vijayaraghavan, R. (1998). *Defence Science Journal, 48*, 155–162.
25. Yang, Y. C., Szafraniec, L. L., Beaudry, W. T., & Way, R. J. (1988). *Journal of Organic Chemistry, 53*, 3293–3297.
26. Shakarjian, M. P., Heck, D. E., Gray, J. P., Sinko, P. J., Gordon, M. K., Casillas, R. P., Heindel, N. D., Gerecke, D. R., Laskin, D. L., & Laskin, J. D. (2010). *Toxicological Sciences, 114*, 5–19.
27. Trompette, J. L., & Meirles, M. (2003). *Journal of Colloid and Interface Science, 263*, 522–527.
28. Allen, L. H., & Matijevic, E. (1970). *Journal of Colloid and Interface Science, 33*, 420–429.
29. Martin, J. E., & Odinek, J. (1992). *Journal of Colloid and Interface Science, 154*, 461–480.
30. Srdic, V., & Radonjic, L. (1992). *Ceramics International, 18*, 73–80.